3 Discretizing

It's a good thing to keep in mind a representative of the family of problems one wishes to model. Here, we shall have wave-propagation problems in view, but heuristic considerations will be based on the much simpler case of static fields. The following example can illustrate both things, depending on whether the exciting current, source of the field, is transient or permanent, and lends itself to other useful variations.

3.1 A model problem

In a closed cavity with metallic walls (Fig. 18), which has been free from any electromagnetic activity till time $t = 0$, suppose a flow of electric charge is created in an enclosed antenna after this instant, by some unspecified agency. An electromagnetic field then develops, propagating at the speed of light towards the walls which, as soon as they are reached by the wavefront, begin to act as secondary antennas. Dielectric or magnetizable bodies inside the cavity, too, may scatter waves. Hence a complex evolution, which one may imagine simulating by numerical means. (How else?)

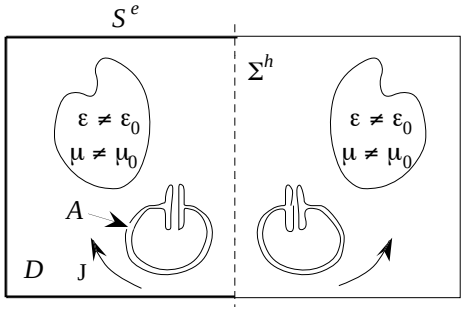

Figure 18. Situation and notation (dimension 3). Region D is the left half of the cavity. Its boundary S has a part S^e in the conductive wall and a part Σ^h in the symmetry plane. Region A, the left "antenna", is the support of the given current density J (mirrored on the right), for which some generator, not represented and not included in the modelling, is responsible.

For the sake of generality, let's assume a symmetry plane, and a symmetrically distributed current. (In that case, the plane acts as a magnetic wall.) The computation will thus be restricted to a spatial domain D coinciding with one half of the cavity, on the left of the symmetry plane, say. Calling S^e and Σ^h, as Fig. 18 shows, the two parts of its surface, an electric wall and a magnetic wall respectively, we write the relevant equations in D as

$$\begin{aligned} \partial_t b + \mathrm{d}e = 0, \qquad & -\partial_t d + \mathrm{d}h = j, \\ d = \epsilon e, \qquad & b = \mu h, \\ \mathrm{t}e = 0 \text{ on } S^e, \qquad & \mathrm{t}h = 0 \text{ on } \Sigma^h. \end{aligned} \tag{26}$$

The coefficients ϵ and μ which generate their Hodge namesakes are real, constant in time, but not necessarily equal to their vacuum values ϵ_0 and μ_0, and may therefore depend on x. (They could even be tensors, as observed earlier.) The current density j is given, and assumed to satisfy $j(t) = 0$ for $t \leq 0$. All fields, besides j, are supposed to be null before $t = 0$, hence initial conditions $e(0) = 0$ and $h(0) = 0$. Notice that $\mathrm{d}j = 0$ is *not* assumed: some electric charge may accumulate at places in the antenna, in accordance with the charge-conservation equation (22).

Proving this problem well-posed[34] is not our concern. Let's just recall that it is so, under reasonable conditions on j, when all fields e and h are constrained to have finite energy.

[34] Its physical relevance has been challenged [92], on the grounds that assuming a given current density (which

Two further examples will be useful. Suppose j has reached a steady value for so long that all fields are now time-independent. The magnetic part of the field, i.e., the pair $\{b, h\}$, can then be obtained by solving, in domain D,

$$\mathrm{d}b = 0, \qquad \mathrm{d}h = j,$$

$$b = \mu h, \tag{27}$$

$$\mathrm{t}b = 0 \text{ on } S^e, \qquad \mathrm{t}h = 0 \text{ on } \Sigma^h.$$

This is also a well-posed problem (magnetostatics), provided $\mathrm{d}j = 0$. As for the electric part of the field, which has no reason to be zero since the asymptotic charge density $q = q(\infty) = -\int_0^\infty \mathrm{d}j(t)\,dt$ does not vanish, as a rule, one will find it by solving

$$\mathrm{d}d = q, \qquad \mathrm{d}e = 0,$$

$$d = \epsilon e, \tag{28}$$

$$\mathrm{t}e = 0 \text{ on } S^e, \qquad \mathrm{t}d = 0 \text{ on } \Sigma^h$$

(electrostatics). The easy task of justifying the boundary conditions in (27) and (28) is left to the reader. One should recognize in (28), thinly veiled behind the present notation, the most canonical example there is of elliptic boundary-value problem.[35]

Finally, let's give an example of eddy-current problem in harmonic regime, assuming a conductivity $\sigma \geq 0$ in D and $\sigma = 0$ in A. This time, all fields are of the form $u(t,x) = \mathrm{Re}[\exp(i\omega t)\,\mathrm{U}(x)]$, with U complex-valued (SMALL CAPITALS will denote such fields). The given current in A, now denoted J^s (s for "source"), is solenoidal, displacement currents are neglected, and Ohm's law $\mathrm{J} = \sigma\mathrm{E} + \mathrm{J}^s$ is in force, where σ is of course understood as a Hodge-like operator, but positive semi-definite only. The problem is then, with the same boundary conditions as above,

$$\mathrm{d}\mathrm{H} = \sigma\mathrm{E} + \mathrm{J}^s, \quad \mathrm{H} = \nu\mathrm{B}, \quad \mathrm{d}\mathrm{E} = -i\omega\mathrm{B},$$

and B and H can be eliminated, hence a second-order equation in terms of E:

$$i\omega\sigma\mathrm{E} + \mathrm{d}\nu\mathrm{d}\,\mathrm{E} = -i\omega\mathrm{J}^s, \tag{29}$$

with boundary conditions $\mathrm{t}\mathrm{E} = 0$ on S^e and $\mathrm{t}\nu\mathrm{d}\mathrm{E} = 0$ on Σ^h.

Nothing forbids σ and μ there to be complex-valued too. (Let's however request them to have Hermitian symmetry.) A complex μ can sometimes serve as a crude but effective way to model ferromagnetic hysteresis. And since the real σ can be replaced by $\sigma + i\omega\epsilon$, we are not committed to drop out displacement currents, after all. Hence, (29) can well be construed as the general version of the Maxwell equations in harmonic regime, at angular frequency ω, with dissipative materials possibly present. In particular, (29) can serve as a model for the "microwave oven" problem. Note that what we have here is a Fredholm equation: Omitting the excitation term J^s and replacing σ by $i\omega\epsilon$ gives the "resonant cavity problem" in D, namely, to find frequencies ω at which $\mathrm{d}\nu\mathrm{d}\,\mathrm{E} = \omega^2\epsilon\mathrm{E}$ has a nonzero solution E.

3.2 Primal mesh

Let's define what we shall call a "cellular paving". This is hardly different from a finite-element mesh, just a bit more general, but we need to be more fussy than is usual about some details.

is routinely done in such problems) neglects the reaction of the antenna to its own radiated field. This is of course true—and there are other simplifications that one might discuss—but misses the point of what *modelling* is about. See [101] and [13], p. 153, for a discussion of this issue.

[35] Mere changes of symbols would yield the stationary heat equation, the equation of steady flow in porous media, etc. Notice in particular how the steady current equation, with Ohm's law, can be written as $\mathrm{d}j = 0, j = \sigma e, \mathrm{d}e = 0$, plus boundary conditions (non-homogeneous, to include source terms).

We pretend to work in n-dimensional Euclidean space E_n, but of course $n = 3$ is the case in point. The cells we use here are those introduced earlier[36] (Fig. 2), with the important caveat that they are all "open" cells, in the sense of §1.2, i.e., do not include their boundaries. (The only exception is for $p = 0$, nodes, which are both open and closed.) The corresponding closed cell will be denoted with an overbar (also used for the topological closure).

This being said, a *cellular paving* of some region R of space is a finite set of open p-cells such that (1) Two distinct cells never intersect, (2) The union of all cells is R, (3) If the closures of two cells c and c' meet, their intersection is the closure of some (unique) cell c''. It may well happen that c'' is c, or c'. In such a case, e.g., if $\overline{c} \cap \overline{c'} = \overline{c}$, we say that c is a *face of* c'. For instance, on Fig. 19, left, c_3 is a face of c_4. If c is a face of c' which itself is a face of c'', then c is a face of c''. Cells in ambient dimension 3 or lower will be called *nodes, edges, facets,* and *volumes*, with symbols n, e, f, v to match.

We'll say we have a *closed* paving if R is closed. (Figure 19, left, gives a two-dimensional example, where $R = \overline{D}$.) But it need not be so. Closed pavings are not necessarily what is needed in practice, as one may rather wish to discard some cells in order to deal with boundary conditions. Hence the relevance of the following notion of "relative closedness": C being a closed part of R, we shall say that a paving of R is *closed modulo* C if it can be obtained by removing, from some closed paving, all the cells which map into C. The case we shall actually need, of a paving of $R = \overline{D} - S^e$ which is closed modulo S^e, is displayed on the right of Fig. 19. Informally said, "pave $\overline{D}$ first, then remove all cells from the electric boundary".

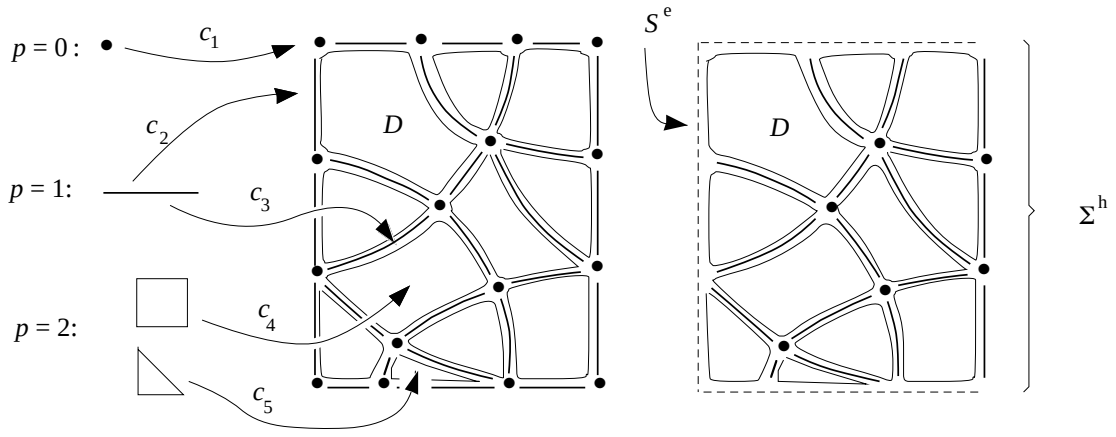

Figure 19. Left: A few p-cells, contributing to a closed cellular paving of D. (This should be imagined in dimension 3.) Right: A culled paving, now "closed relative to" S^e. This is done in anticipation of the modelling we have in mind, in which cells of S^e would carry null degrees of freedom, so they won't be missed.

Each cell has its own inner orientation. These orientations are arbitrary and independent. In three dimensions, we shall denote by $\mathcal{N}, \mathcal{E}, \mathcal{F}, \mathcal{V}$, the sets of oriented p-cells of the paving, and by N, E, F, V the number of cells in each of these sets. (The general notation, rarely required, will be $\mathcal{S}_p$ for the set of p-cells and S_p for the number of such cells.)

Two cells σ and c, of respective dimensions p and $p+1$, are assigned an *incidence number*, equal to ± 1 if σ is a face of c, and to 0 otherwise. As for the sign, recall that each cell orients its own boundary (§1.4), so this orientation may or may not coincide with the one attributed to σ. If orientations match, the sign is $+$, else it's $-$. Figure 20 illustrates this point. (Also refer back to Fig. 10.)

Collecting these numbers in arrays, we obtain rectangular matrices **G, R, D**, called *incidence matrices* of the tesselation. For instance (Fig. 20), the incidence number for edge e and facet f is denoted $\mathbf{R}^e_f$, and makes one entry in matrix **R**, whose rows and columns are

[36] Topologically simple *smooth* cells, therefore. But the latter condition is not strict and we shall relax it to *piecewise* smooth, in the sequel, without special warning.

indexed over facets and edges, respectively. The entry $\mathbf{G}_e^n$ of $\mathbf{G}$ is -1 in the case displayed, because n, positively oriented, is at the start of edge e (cf. Fig. 6*c*). And so on. Symbols **G, R, D** are of course intentionally reminiscent of grad, rot, div, but we still have a long way to go to fully understand the connection. Yet, one thing should be conspicuous already: contrary to grad, rot, div, the incidence matrices are *metric-independent* entities, so the analogy cannot be complete. Matrices **G**, **R**, **D** are more akin to the (metric-independent) operator d from this viewpoint, and the generic symbol **d**, indexed by the dimension p if needed, will make cleaner notation in spatial dimensions higher than 3, with $\mathbf{d}_0 = \mathbf{G}$, $\mathbf{d}_1 = \mathbf{R}$, $\mathbf{d}_2 = \mathbf{D}$. The mnemonic value of **G**, **R**, **D**, however, justifies keeping them in use.

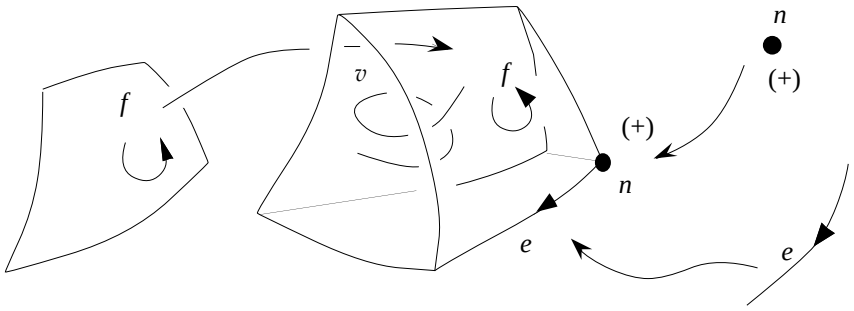

Figure 20. Sides: Individual oriented cells. Middle: The same, plus a 3-cell, as part of a paving, showing respective orientations. Those of v and f match, those of f and e, or of e and n, don't. So $\mathbf{G}_e^n = -1$, $\mathbf{R}_f^e = -1$, and $\mathbf{D}_v^f = 1$.

Just as $\mathrm{rot} \circ \mathrm{grad} = 0$ and $\mathrm{div} \circ \mathrm{rot} = 0$, one has $\mathbf{GR} = 0$ and $\mathbf{DR} = 0$. Indeed, for an edge e and a volume v, the $\{v, e\}$-entry of $\mathbf{DR}$ is $\sum_{f \in \mathcal{F}} \mathbf{D}_v^f \mathbf{R}_f^e$. Nonzero terms occur, in this sum over facets, only for those which both contain e and are a face of v, which happens only if e belongs to $\overline{v}$. In that case, there are exactly two facets f and g of v meeting along e (Fig. 21), and hence two nonzero terms. As Fig. 21 shows, they have opposite signs, whatever the orientations of the individual cells, hence the result, $\mathbf{DR} = 0$. By a similar argument, $\mathbf{RG} = 0$, and more generally, $\mathbf{d}_{p+1}\mathbf{d}_p = 0$.

Remark. The answer to the natural question, "then, is the kernel of **R** equal to the range of **G** ?", is "yes" here, because $\overline{D} - S^e$ has simple topology. (See the Remark at the end of §1.4 about homology. This time, going further would lead us into *co*homology.) For the same reason, $\ker(\mathbf{D}) = \mathrm{cod}(\mathbf{R})$. This will be important below. ♢

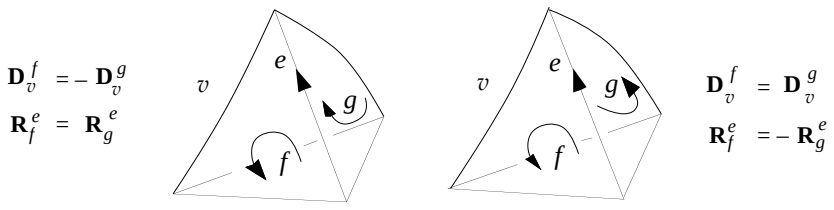

Figure 21. Relation $\mathbf{DR} = 0$, and how it doesn't depend on the cells' individual orientations: In both cases, one has $\mathbf{D}_v^f \mathbf{R}_f^e + \mathbf{D}_v^g \mathbf{R}_g^e = 0$.

It is no accident if this proof of $\mathbf{d} \circ \mathbf{d} = 0$ evokes the one about $\partial \circ \partial = 0$ in §1.4, and the caption of Fig. 10. The same basic observation, "the boundary of a boundary is zero" [96, 58], underlies all proofs of this kind. In fact, the above incidence matrices can be used to find the boundaries, chainwise, of each cell. For instance, f being understood as the 2-chain based on facet f with weight 1, one has $\partial f = \sum_{e \in \mathcal{E}} \mathbf{R}_f^e \, e$. So if S is the straight 2-chain $\sum_f w^f f$ with weights w^f (which we shall call a *primal 2-chain*, or "m-surface", using m as a mnemonic for

the underlying mesh), its boundary[37] is the 1-chain

$$\partial S = \sum_{e\in\mathcal{E}} \sum_{f\in\mathcal{F}} \mathbf{R}_f^e w^f \, e. \tag{30}$$

More generally, let's write $\boldsymbol{\partial}_p$, boldface,[38] for the transpose of the above matrix $\mathbf{d}_{p-1}$. Then, if $c = \sum_{\sigma\in\mathcal{S}_p} w^\sigma \sigma$ is a p-chain, its boundary is $\partial c = \sum\{s \in \mathcal{S}_{p-1} : (\boldsymbol{\partial}_p \mathbf{w})^s \, s\}$, where $\mathbf{w}$ stands for the vector of weights. Thus, $\boldsymbol{\partial}$ is to ∂ what $\mathbf{d}$ is to d. Moreover, the duality between d and ∂ is matched by a similar duality between their finite-dimensional counterparts $\mathbf{d}$ and $\boldsymbol{\partial}$.

3.3 Dual mesh

The *dual* mesh of D is also a cellular paving, though not of the same region exactly, and with *outer* orientation of cells. Let's explain.

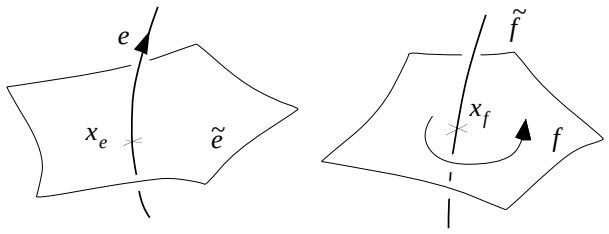

Figure 22. Inner orientations of edge e and facet f, respectively, give crossing direction through $\check{e}$ and gyratory sense around $\check{f}$.

To each p-cell c of the primal mesh, we assign a unique $(n-p)$-cell, called the *dual* of c and denoted $\check{c}$, which meets c at a single point x_c. Hence a one-to-one correspondence between cells of complementary dimensions. Thus, for instance, facet f is pierced by the dual edge $\check{f}$ (a line), node n is inside the dual volume $\check{n}$, and so forth. Since the tangent spaces at x_c to c and $\check{c}$ are complementary, the inner orientation of c provides an outer orientation for $\check{c}$ (Fig. 22). Incidence matrices $\tilde{\mathbf{G}}, \tilde{\mathbf{R}}, \tilde{\mathbf{D}}$ can then be defined, as above, the sign of each nonzero entry depending on whether outer orientations match or not.

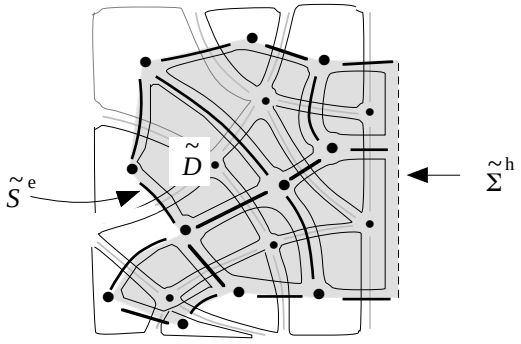

Figure 23. A dual paving, overlaid on the primal one.

Moreover, it is required that, when c is a face of c', the dual $\check{c}'$ be a face of $\check{c}$, and the other way round. This has two consequences. First, we don't really need new names for the dual incidence matrices. Indeed, consider for instance edge e and facet f, and suppose $\mathbf{R}_f^e = 1$, i.e., e is a face of f and their orientations match: Then the dual edge $\check{f}$ is a face of the dual facet $\check{e}$, whose outer orientations match, too. So what we would otherwise denote $\tilde{\mathbf{R}}_{\check{e}}^{\check{f}}$ is equal to $\mathbf{R}_f^e$. Same equality if $\mathbf{R}_f^e = -1$, and same reasoning for other kinds of cells, from which we conclude that the would-be dual incidence matrices $\tilde{\mathbf{G}}, \tilde{\mathbf{R}}, \tilde{\mathbf{D}}$ are just the transposes $\mathbf{D}^t, \mathbf{R}^t, \mathbf{G}^t$ of the primal ones.

[37] More accurately, its boundary *relative to* Σ^h.

[38] Boldface, from now on, connotes mesh-related things, such as DoF arrays, etc.

Second consequence, there is no gap between dual cells, which thus form a cellular paving of a connected region $\check{R}$, the interior $\check{D}$ of which is nearly D, but not quite (Fig. 23). A part of its boundary is paved by dual cells: We name it $\check{S}^e$, owing to its kinship with S^e (not so obvious on our coarse drawing! but the finer the mesh, the closer $\check{S}^e$ and S^e will get). The other part is denoted $\check{\Sigma}^h$. So the cellular paving we now have is closed modulo $\check{\Sigma}^h$, whereas the primal one was closed modulo S^e.

Given the mesh m, all its conceivable duals have the same *combinatorial* structure (the same incidence matrices), but can differ as regards *metric*, which leaves much leeway to construct dual meshes. Two approaches are noteworthy, which lead to the "barycentric dual" and the "Voronoi–Delaunay dual". We shall present them as special cases of two slightly more general procedures, the "star construction" and the "orthogonal construction" of meshes in duality. For this we shall consider only *polyhedral* meshes (those with polyhedral 3-cells), which is not overly restrictive in practice.

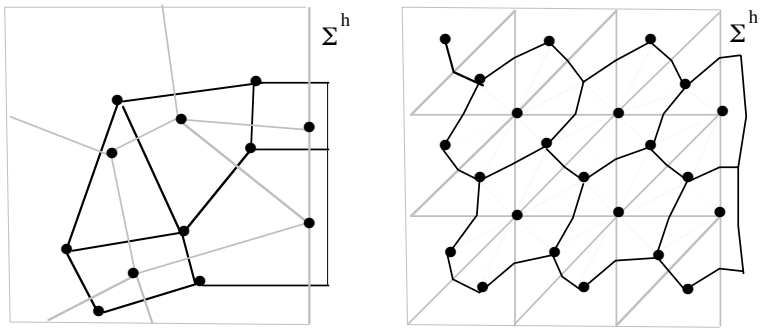

Figure 24. Left: Orthogonal dual mesh. (Same graphic conventions as in Fig. 23, slightly simplified.) Right: Star construction of a dual mesh (close enough, here, to a barycentric mesh, but not quite the same). Notice the isolated dual edge, and the arbitrariness in shaping dual cells beyond Σ^h.

The orthogonal construction consists in having each dual cell orthogonal to its primal partner. (Cf. Figs 24 and 26, left.) A particular case is the Voronoi–Delaunay tesselation [33], under the condition that dual nodes should be inside primal volumes. Alas, as Fig. 25 shows, orthogonality can be impossible to satisfy, if the primal mesh is imposed. If one starts from a simplicial primal for which all circumscribed spheres have their center inside the tetrahedron, all goes well. (One then takes these circumcenters as dual nodes.) But this property, desirable on many accounts, is not so easily obtained, and certainly not warranted by common mesh generators.

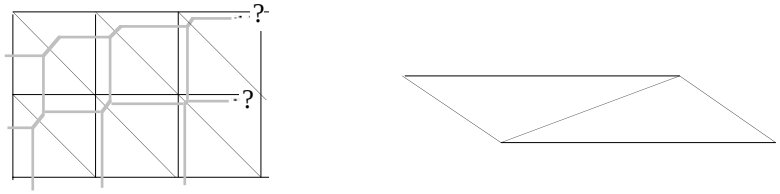

Figure 25. Left: How hopeless the orthogonal construction can become, even with a fairly regular primal mesh. Right: Likely the simplest example of a 2D mesh without any orthogonal dual.

Hence the usefulness of the star construction, more general, because it applies to any primal mesh with star-shaped cells. A part A of A_n is *star-shaped* if it contains a point a, that we shall call a *center*, such that the whole segment $[a, x]$ belongs to A when x belongs to A. Now, pick such a center in each primal cell (the center of a primal node is itself), and join it to centers of all faces of the cell. This way, *simplicial* subcells are obtained (tetrahedra and their faces, in 3D). One gets the dual mesh by rearranging them, as follows: for each primal cell c, build its dual by putting together all k-subcells, $k \leq n - p$, which have one of their vertices at c's center, and other vertices at centers of cells incident on c. Figures 24 and 26, right, give the idea. If all primal cells are simplices to start with, taking the barycenters of their faces as

centers will give the *barycentric* dual mesh evoked a bit earlier.

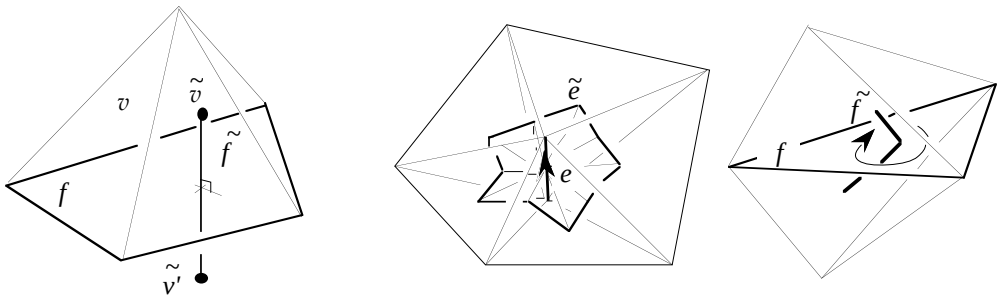

Figure 26. Left: A facet f and its dual edge $\tilde{f}$ in the orthogonal construction ($\tilde{v}$ and $\tilde{v}'$ are the dual nodes which lie inside the volumes v and v' just above and just below f). From $\tilde{v}$, all boundary facets of v can directly be seen at right angle, but we don't require more: $\tilde{v}$ is neither v's barycenter nor the center of its circumscribed sphere, if there is such a sphere. Right: A dual facet and a dual edge, in the case of a simplicial primal mesh and of its barycentric dual. Observe the orientations.

Remark. The recipe is imprecise about cells dual to those of Σ^h, whose shape outside D can be as one fancies (provided the requirements about duality are satisfied). Nothing there to worry about: Such choices are just as arbitrary as the selection of the centers of cells. It's all part of the unavoidable approximation error, which can be reduced at will by refinement.[39] ♢

Remark. If, as suggested above ("pave $\overline{D}$ first ..."), the primal mesh has been obtained by culling from a closed one, subcells built from the latter form a refinement of *both* the primal mesh and the dual mesh. The existence of this common "underlying simplicial complex" will be an asset when designing finite elements. ♢

3.4 A discretization kit

We are ready, now, to apply the afore-mentioned strategy: Satisfy the balance equations (15) and (17) for a selected *finite* family of surfaces.

Let's first adopt a finite, approximate representation of the fields. Consider b, for instance. As a 2-form, it is meant to be integrated over inner oriented surfaces. So one may consider the integrals $\int_f b$, denoted $\mathbf{b}_f$, for all facets f, as a kind of "sampling" of b, and take the array of such "degrees of freedom" (DoF), $\{\mathbf{b} = \mathbf{b}_f : f \in \mathcal{F}\}$, indexed over primal facets, as a finite representation of b. This does not tell us about the *value* of the field at any given point, of course. But is that the objective? Indeed, all we know about a field is what we can measure, and we don't measure point values. These are abstractions. What we do measure is, indirectly, the *flux* of b, embraced by the loop of a small enough magnetic probe, by reading off the induced e.m.f. The above sampling thus consists in having each facet of the mesh play the role of such a probe, and the smaller the facets, the better we know the field. Conceivably, the mesh may be made so fine that the $\mathbf{b}_f$'s are *sufficient information* about the field, in practice. (Anyway, we'll soon see how to compute an approximation of the flux for any surface, knowing the $\mathbf{b}_f$'s.) So one may be content with a method that would yield the four meaningful arrays of degrees of freedom, listing

- the edge e.m.f.'s, $\mathbf{e} = \{\mathbf{e}_e : e \in \mathcal{E}\}$,
- the facet fluxes, $\mathbf{b} = \{\mathbf{b}_f : f \in \mathcal{F}\}$,
- the dual-edge m.m.f.'s, $\mathbf{h} = \{\mathbf{h}_f : f \in \mathcal{F}\}$,
- and the dual-facet displacement currents, $\mathbf{d} = \{\mathbf{d}_e : e \in \mathcal{E}\}$,

all that from a similar sampling, across dual facets, of the given current j, encoded in the DoF array $\mathbf{j} = \{\mathbf{j}_e : e \in \mathcal{E}\}$.

[39] A *refinement* of a paving is another paving of the same region, which restricts to a proper cellular paving of each original cell.

In this respect, considering the integral form (15) and (17) of the basic equations will prove much easier than dealing with so-called "weak forms" of the infinitesimal equations (16) and (18). In fact, this simple shift of emphasis (which is the gist of Weiland's "finite integration theory" [103] and of Tonti's "cell method" [99, 65]) will so to speak *force on us* the right and unique discretization, as follows.

3.4.1 Network equations, discrete Hodge operator

Suppose the chain S in (15) is the simplest possible in the present context, that is, a *single* primal facet, f. The integral of e along ∂f is the sum of its integrals along edges that make ∂f, with proper signs, which are precisely the signs of the incidence numbers, by their very definition. Therefore, eq. (15) applied to f yields

$$\partial_t \mathbf{b}_f + \sum_{e \in \mathcal{E}} \mathbf{R}^e_f \mathbf{e}_e = 0.$$

There is one equation like this for each facet of the primal mesh, that is—thanks for having discarded facets in S^e, for which the flux is known to be 0—one for each genuinely unknown facet-flux of b. Taken together, in matrix form,

$$\partial_t \mathbf{b} + \mathbf{R}\mathbf{e} = 0, \tag{31a}$$

they form the first group of our *network* differential *equations*.

The same reasoning about each dual facet $\tilde{e}$ (the simplest possible outer-oriented surface that Σ in (17) can be) yields

$$-\partial_t \mathbf{d}_e + \sum_{f \in \mathcal{F}} \mathbf{R}^e_f \mathbf{h}_f = \mathbf{j}_e,$$

for all e in $\mathcal{E}$, i.e., in matrix form,

$$-\partial_t \mathbf{d} + \mathbf{R}^t \mathbf{h} = \mathbf{j}, \tag{31b}$$

the second group of network equations.

To complete this system, we need discrete counterparts to $b = \mu h$ and $d = \epsilon e$, i.e., *network constitutive laws,* of the form

$$\mathbf{b} = \boldsymbol{\mu}\mathbf{h}, \qquad \mathbf{d} = \boldsymbol{\epsilon}\,\mathbf{e}, \tag{32}$$

where $\boldsymbol{\epsilon}$ and $\boldsymbol{\mu}$ are appropriate square symmetric matrices. Understanding how such matrices can be built is our next task. It should be clear that no *canonical* construction can exist—for sure, nothing comparable to the straightforward passage from (15)(17) to (31a)(31b)—because the metric of both meshes must intervene (eq. (19) gives a clue in this respect). Indeed, the exact equivalent of (31), up to notational details, can be found in most published algorithms (including those based on the Galerkin method, see e.g., [62]), whereas a large variety of proposals exist as regards $\boldsymbol{\epsilon}$ and $\boldsymbol{\mu}$. These "discrete Hodge operators" are the real issue. Constructing "good" ones, in a sense we still have to discover, is the central problem.

Our approach will be as follows: First—just not to let the matter dangling too long—we shall give *one* solution, especially simple, to this problem, which makes $\boldsymbol{\epsilon}$ and $\boldsymbol{\mu}$ *diagonal*, a feature the advantages of which we shall appreciate by working out a few examples. Later (in Section 4), a generic error analysis method will be sketched, from which a *criterion* as to what makes a good $\boldsymbol{\epsilon}$–$\boldsymbol{\mu}$ pair will emerge. Finite elements will enter the stage during this process, and help find other solutions to the problem, conforming to the criterion.

The simple solution is available if one has been successful in building a dual mesh by the orthogonal construction (Figs 24 and 26, left). Then, in the case when ϵ and μ are uniform, one sets $\boldsymbol{\epsilon}^{ee'} = 0$ if $e \neq e'$, $\boldsymbol{\mu}^{ff'} = 0$ if $f \neq f'$, and (cf. (19))

$$\boldsymbol{\epsilon}^{ee} = \epsilon \frac{\text{area}(\tilde{e})}{\text{length}(e)}, \quad \boldsymbol{\mu}^{ff} = \mu \frac{\text{area}(f)}{\text{length}(\tilde{f})}, \tag{33}$$

which does provide diagonal matrices $\boldsymbol{\epsilon}$ and $\boldsymbol{\mu}$. (The inverse of $\boldsymbol{\mu}$ will be denoted by $\boldsymbol{\nu}$.) The heuristic justification [99] is that *if* the various fields happened to be piecewise constant (relative to the primal mesh), formulas (33) would exactly correspond to the very definition (19) of the Hodge operator. (Section 4.1 will present a stronger argument.) In the case of non-uniform coefficients, formulas such as

$$\boldsymbol{\mu}^{ff} = \frac{\mu_1 \mu_2 \,\mathrm{area}(f)}{\mu_2 \mathrm{length}(\tilde{f}_1) + \mu_1 \mathrm{length}(\tilde{f}_2)}, \tag{34}$$

where $\tilde{f}_1$ and $\tilde{f}_2$ are the parts of $\tilde{f}$ belonging to the two volumes adjacent to f, apply instead (Fig. 27). Observe the obvious intervention of metric elements (lengths, areas, angles) in these constructions.

Remark. Later, when edge elements w^e and facet elements w^f will enrich the toolkit, we shall consider another solution, that consists in setting $\boldsymbol{\epsilon}^{ee'} = \int_D \epsilon w^e \wedge w^{e'}$ and $\boldsymbol{\nu}^{ff'} = \int_D \mu^{-1} w^f \wedge w^{f'}$. For reference, let's call this the "Galerkin approach" to the problem. We shall use loose expressions such as "the Galerkin $\boldsymbol{\epsilon}$", or "the diagonal hodge", to refer to various brands of discrete Hodge operators. ◊

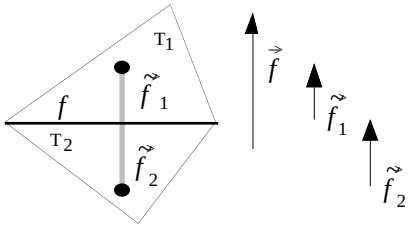

Figure 27. The case of a discontinuous permeability (μ_1 and μ_2 in primal volumes T_1 and T_2, separated by facet f). We denote by $\vec{f}$ the vectorial area of f and by $\vec{\tilde{f}}_1, \vec{\tilde{f}}_2$, the vectors along both parts of $\tilde{f}$. Let u and v be arbitrary vectors, respectively normal and tangent to f, and let $\mathrm{H}_1 = u + v$ in T_1. Transmission conditions across f determine a unique uniform field $\mathrm{B}_2 = \mu_1 u + \mu_2 v$ in T_2. Then $\mathbf{b}_f = \mu_1 \vec{f} \cdot u$ and $\mu_2 \mathbf{h}_f = \mu_2 \vec{\tilde{f}}_1 \cdot u + \mu_1 \vec{\tilde{f}}_2 \cdot u$. As $\vec{f}$, $\vec{\tilde{f}}_1$, and $\vec{\tilde{f}}_2$ are collinear, u disappears from the quotient $\mathbf{b}_f / \mathbf{h}_f$, yielding (34).

3.4.2 The toolkit

At this stage, we have obtained discrete counterparts (Fig. 28) to most features of the "Maxwell building" of Fig. 17, but time differentiation and wedge product still miss theirs. Some thought about how the previous ideas would apply in four dimensions should quickly suggest the way to deal with time derivatives: δt being the time step, call $\mathbf{b}^k$, $\mathbf{h}^k$, the values of $\mathbf{b}$, $\mathbf{h}$ at time $k\delta t$, for $k = 0, 1, \ldots$, call $\mathbf{j}^{k+1/2}$, $\mathbf{d}^{k+1/2}$, $\mathbf{e}^{k+1/2}$ those of $\mathbf{j}$, $\mathbf{d}$, $\mathbf{e}$ at time $(k + 1/2)\delta t$, and approximate $\partial_t \mathbf{b}$, at time $(k + 1/2)\delta t$, by $(\mathbf{b}^{k+1} - \mathbf{b}^k)/\delta t$, and similarly, $\partial_t \mathbf{d}$, now at time $k\delta t$, by $(\mathbf{d}^{k+1/2} - \mathbf{d}^{k-1/2})/\delta t$.

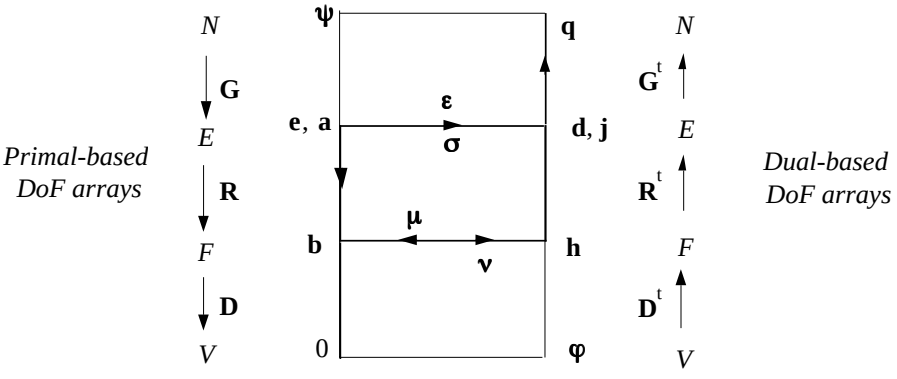

Figure 28. A "discretization toolkit" for Maxwell's equations

As for the wedge product, to $\int_D b \wedge h$ corresponds the sum $\Sigma_{f \in \mathcal{F}} \mathbf{b}_f \mathbf{h}_f$, which we shall denote by $(\mathbf{b}, \mathbf{h})$, with bold parentheses. Similarly, $\int_D d \wedge e$ corresponds to $\Sigma_{e \in \mathcal{E}} \mathbf{d}_e \mathbf{e}_e$, also

denoted $(\mathbf{d},\mathbf{e})$. Hence we may define "discrete energy" quadratic forms, $\frac{1}{2}(\boldsymbol{\nu}\mathbf{b},\mathbf{b})$, $\frac{1}{2}(\boldsymbol{\mu}\mathbf{h},\mathbf{h})$, $\frac{1}{2}(\boldsymbol{\epsilon}\,\mathbf{e},\mathbf{e})$, and $\frac{1}{2}(\boldsymbol{\epsilon}^{-1}\mathbf{d},\mathbf{d})$, all quantities with, indeed, the physical dimension of energy (but be aware that $(\mathbf{j},\mathbf{e})$ is a power instead, like $\int_D j\wedge e$). Some notational shortcuts: Square roots such as $(\boldsymbol{\nu}\mathbf{b},\mathbf{b})^{1/2}$, or $(\boldsymbol{\epsilon}\,\mathbf{e},\mathbf{e})^{1/2}$, etc., will be denoted by $\|\mathbf{b}\|_\nu$, or $|\mathbf{e}|_\epsilon$, in analogy with the above $|b|_\nu$, or $|e|_\epsilon$, and serve as various, physically meaningful *norms* on the vector spaces of DoF arrays. We'll say the "ν-norm", the "ϵ-norm", etc., for brevity.

Proposition 3. *If equations* (31–32) *are satisfied, one has*

$$d_t\left[\tfrac{1}{2}(\boldsymbol{\nu}\mathbf{b},\mathbf{b})+\tfrac{1}{2}(\boldsymbol{\epsilon}\,\mathbf{e},\mathbf{e})\right]=-(\mathbf{j},\mathbf{e}). \tag{35}$$

Proof. Take the bold scalar product of (31a) and (31b) by $\mathbf{h}$ and $-\mathbf{e}$, add, and use the equality $(\mathbf{R}\mathbf{e},\mathbf{h})=(\mathbf{e},\mathbf{R}^t\mathbf{h})$. ♢

Remark. The analogue of $\int_S h\wedge e$, when S is some m-surface, is $\Sigma_{f\in\mathcal{F}(S),e\in\mathcal{E}}\mathbf{R}^e_f\mathbf{h}_f\mathbf{e}_e$, where $\mathcal{F}(S)$ stands for the subset of facets which compose S. (Note how this sum vanishes if S is the domain's boundary.) By exploiting this, the reader will easily modify (35) in analogy with the Poynting theorem. In spite of such formal correspondences, energy and discrete energy have, a priori, no relation. To establish one, we shall need "interpolants", such as finite elements, enabling us to pass from degrees of freedoms to fields. For instance, facet elements will generate a mapping $\mathbf{b}\to b$, with $b=\Sigma_f\mathbf{b}_f w^f$. If $\boldsymbol{\nu}$ is the Galerkin hodge, then $\int_D \nu b\wedge b=(\boldsymbol{\nu}\mathbf{b},\mathbf{b})$. Such built-in equality between energy and discrete energy is an exception, a distinctive feature of the Ritz–Galerkin approach. With other discrete hodges, even *convergence* of discrete energy, as the mesh is refined, towards the true one, should not be expected. ♢

3.5 Playing with the kit: Full Maxwell

Now we have enough to discretize any model connected with Maxwell's equations. Replacing, in (26), rot by $\mathbf{R}$ or $\mathbf{R}^t$, ϵ and μ by $\boldsymbol{\epsilon}$ and $\boldsymbol{\mu}$, and ∂t by the integral or half-integral differential quotient, depending on the straight or twisted nature of the differential formin consideration, we obtain this:

$$\frac{\mathbf{b}^{k+1}-\mathbf{b}^k}{\delta t}+\mathbf{R}\mathbf{e}^{k+1/2}=0,\qquad -\boldsymbol{\epsilon}\,\frac{\mathbf{e}^{k+1/2}-\mathbf{e}^{k-1/2}}{\delta t}+\mathbf{R}^t\boldsymbol{\nu}\mathbf{b}^k=\mathbf{j}^k \tag{36}$$

(where $\mathbf{j}^k$ is the array of intensities through dual facets, at time[40] $k\delta t$), with initial conditions

$$\mathbf{b}^0=0,\quad \mathbf{e}^{-1/2}=0. \tag{37}$$

In the simplest case where the primal and dual mesh are plain rectangular staggered grids, (36)(37) is the well known Yee scheme [111]. So what we have here is the closest thing to Yee's scheme in the case of *cellular* meshes.

A similar numerical behavior can therefore be expected. Indeed,

Proposition 4. *The scheme* (36)(37) *is stable for δt small enough, provided both $\boldsymbol{\epsilon}$ and $\boldsymbol{\nu}$ are symmetric positive definite.*

Proof. For such a proof, one may assume $\mathbf{j}=0$ and nonzero initial values in (37), satisfying $\mathbf{D}\mathbf{b}^0=0$. Eliminating $\mathbf{e}$ from (36), one finds that

$$\mathbf{b}^{k+1}-2\mathbf{b}^k+\mathbf{b}^{k-1}+(\delta t)^2\mathbf{R}\boldsymbol{\epsilon}^{-1}\mathbf{R}^t\boldsymbol{\nu}\mathbf{b}^k=0. \tag{38}$$

Since $\mathbf{D}\mathbf{R}=0$, the "loop invariant" $\mathbf{D}\mathbf{b}^k=0$ holds, so one may work in the corresponding subspace, $\ker(\mathbf{D})$. Let's introduce the (generalized) eigenvectors $\mathbf{v}_i$ such that $\mathbf{R}\boldsymbol{\epsilon}^{-1}\mathbf{R}^t\mathbf{v}_i=\lambda_i\boldsymbol{\mu}\mathbf{v}_i$, which satisfy $(\boldsymbol{\mu}\mathbf{v}_i,\mathbf{v}_j)=1$ if $i=j$, 0 if $i\neq j$. In this "μ-orthogonal" basis, $\mathbf{b}^k=\boldsymbol{\mu}\Sigma_i\eta_i^k\mathbf{v}_i$, and (38) becomes

$$\eta_i^{k+1}-(2-\lambda_i(\delta t)^2)\eta_i^k+\eta_i^{k-1}=0$$

[40] For easier handling of Ohm's law, $\mathbf{j}(k\delta t)$ may be replaced by $(\mathbf{j}^{k+1/2}+\mathbf{j}^{k-1/2})/2$.

for all i. The η_i^ks, and hence the $\mathbf{b}^k$s, stay bounded if the characteristic equation of each of these recurrences has imaginary roots, which happens (Fig. 29) if $0 < \lambda_j \delta t < 2$ for all j. $\diamondsuit$

In the case of the original Yee scheme, eigenvalues could explicitly be found, hence the well-know relation [111] between the maximum possible value of δt and the lengths of the cell sides. For general grids, we have no explicit formulas, but the thumbrule is the same: δt should be small enough for a signal travelling at the speed of light (in the medium under study) not to cross more than one cell during this lapse of time.

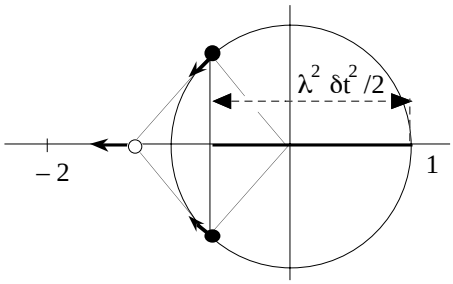

Figure 29. The white spot lies at the sum of roots of the characteristic equation $r^2 - (2 - \lambda_i(\delta t)^2)r + 1 = 0$. Stability is lost if it leaves the interval $[-2, 2]$.

This stringent stability condition makes the scheme unattractive if not fully explicit, or nearly so: $\boldsymbol{\epsilon}$ should be *diagonal*, or at the very least, block-diagonal with most blocks of size 1 and a few small-size ones, and $\boldsymbol{\nu}$ should be sparse. If so is the case, each time step will only consist in a few matrix–vector products plus, perhaps, the resolution of a few small linear systems, which makes up for the large number of time steps. Both conditions are trivially satisfied with the orthogonal construction (cf. (33)(34)), but we have already noticed the problems this raises. Hence the sustained interest for so-called "mass-lumping" procedures, which aim at replacing the Galerkin $\boldsymbol{\epsilon}$ by a diagonal matrix without compromising convergence [48], [26], [38]. (See [19] for a coordinate-free reinterpretation of [48].)

Remark. Obviously, there is another version of the scheme, in $\mathbf{h}$ and $\mathbf{d}$, for which what is relevant is sparsity of $\boldsymbol{\epsilon}^{-1}$ and diagonality of $\boldsymbol{\mu}$, i.e., of $\boldsymbol{\nu}$. Unfortunately, the diagonal lumping procedure that worked for edge elements fails whan applied to the Galerkin $\boldsymbol{\nu}$, i.e., to the mass-matrix of facet elements [19]. $\diamondsuit$

There are of course other issues than stability to consider, but we shall not dwell on them right now. For *convergence* (to be treated in detail later, but only in statics), cf. [70], [75], [19]. On *dispersion* properties, little can be said unless the meshes have some translational and rotational symmetry, at least locally, and this is beyond our scope. As for *conservation* of some quantities, it would be nice to be able to say, in the case when $\mathbf{j} = 0$, that "total discrete energy is conserved", but this is only almost true. Conserved quantities, as one will easily verify, are $\frac{1}{2}(\boldsymbol{\mu}\mathbf{h}^{k+1}, \mathbf{h}^k) + \frac{1}{2}(\boldsymbol{\epsilon}\,\mathbf{e}^{k+\frac{1}{2}}, \mathbf{e}^{k+\frac{1}{2}})$ and $\frac{1}{2}(\boldsymbol{\mu}\mathbf{h}^k, \mathbf{h}^k) + \frac{1}{2}(\boldsymbol{\epsilon}\,\mathbf{e}^{k-\frac{1}{2}}, \mathbf{e}^{k+\frac{1}{2}})$, both independent of k. So their half-sum, which can suggestively be written as

$$W_k = \tfrac{1}{2}(\boldsymbol{\mu}\mathbf{h}^{k+\frac{1}{2}}, \mathbf{h}^k) + \tfrac{1}{2}(\boldsymbol{\epsilon}\,\mathbf{e}^k, \mathbf{e}^{k+\frac{1}{2}}),$$

if one agrees on $\mathbf{h}^{k+\frac{1}{2}}$ and $\mathbf{e}^k$ as shorthands for $[\mathbf{h}^k + \mathbf{h}^{k+1}]/2$ and $[\mathbf{e}^{k-\frac{1}{2}} + \mathbf{e}^{k+\frac{1}{2}}]/2$, is conserved: *Not* the discrete energy, definitely, however close.

3.6 Playing with the kit: Statics

Various discrete models can be derived from (36) by the usual maneuvers (neglect the displacement current term $\boldsymbol{\epsilon}\,\mathbf{e}$, omit time-derivatives in static situations), but it may be more instructive to obtain them from scratch. Take the magnetostatic model (27), for instance: Replace forms b and h by the DoF arrays $\mathbf{b}$ and $\mathbf{h}$, the d by the appropriate matrix, as read off from Fig. 28, and obtain

$$\mathbf{D}\mathbf{b} = 0, \quad \mathbf{h} = \boldsymbol{\nu}\mathbf{b}, \quad \mathbf{R}^t\mathbf{h} = \mathbf{j}, \tag{39}$$

which automatically includes the boundary conditions, thanks for having discarded[41] "passive" boundary cells. Observe that $\mathbf{G}^t\mathbf{j} = 0$ must hold for a solution to exist: But this is the discrete counterpart, as Fig. 28 shows, of $\mathrm{d}j = 0$, i.e., of $\operatorname{div} \mathrm{J} = 0$ in vector notation.

In the next Section, we shall study the convergence of (39). When it holds, all schemes equivalent to (38) that can be obtained by algebraic manipulations are thereby equally valid—and there are lots of them. First, let $\mathbf{h}^\mathbf{j}$ be one of the facet-based arrays[42] such that $\mathbf{R}^t\mathbf{h}^\mathbf{j} = \mathbf{j}$. Then $\mathbf{h}$ in (39) must be of the form $\mathbf{h} = \mathbf{h}^\mathbf{j} + \mathbf{D}^t\boldsymbol{\varphi}$. Hence (39) becomes

$$\mathbf{D}\boldsymbol{\mu}\mathbf{D}^t\boldsymbol{\varphi} = -\mathbf{D}\boldsymbol{\mu}\mathbf{h}^\mathbf{j}. \tag{40}$$

This, which corresponds to $-\operatorname{div}(\mu(\operatorname{grad}\Phi + \mathrm{H}^j)) = 0$, the scalar potential formulation of magnetostatics, is not interesting unless $\boldsymbol{\nu}$ is diagonal, or nearly so, since $\boldsymbol{\mu}$ is full otherwise. So it requires the orthogonal construction, and is not an option in the case of the Galerkin $\boldsymbol{\nu}$. It's a well-studied scheme [7, 30, 42, 49, 53, 94], called "block-centered" in other sectors of numerical engineering [56, 106], because degrees of freedom, assigned to the *dual* nodes, appear as lying inside the primal volumes, or "blocks". Uniqueness of $\boldsymbol{\varphi}$ is easily proved,[43] which implies the uniqueness—not so obvious, a priori—of $\mathbf{h}$ and $\mathbf{b}$ in (39).

Symmetrically, there is a scheme corresponding to the vector potential formulation (i.e., $\operatorname{rot}(\nu \operatorname{rot} \mathrm{A}) = \mathrm{J}$):

$$\mathbf{R}^t\boldsymbol{\nu}\mathbf{R}\mathbf{a} = \mathbf{j}, \tag{41}$$

obtained by setting $\mathbf{b} = \mathbf{R}\mathbf{a}$, where the DoF array $\mathbf{a}$ is indexed over (active) edges. (If $\boldsymbol{\nu}$ is the Galerkin hodge, (41) is what one obtains when using edge elements to represent the vector potential.) Existence in (41) stems from $\mathbf{G}^t\mathbf{j} = 0$. No uniqueness this time, because $\ker(\mathbf{R})$ does not reduce to 0, but all solutions $\mathbf{a}$ give the same $\mathbf{b}$, and hence the same $\mathbf{h} = \boldsymbol{\nu}\mathbf{b}$.

Remark. Whether to "gauge" $\mathbf{a}$ in this method, that is, to impose a condition that would select a unique solution, such as $\mathbf{G}^t\boldsymbol{\epsilon}\,\mathbf{a} = 0$ for instance, remains to these days a contentious issue. It depends on which method is used to solve (41), and on how well the necessary condition $\mathbf{G}^t\mathbf{j} = 0$ is implemented. With iterative methods such as the conjugate gradient and its variants, and if one takes care to use $\mathbf{R}^t\mathbf{h}^\mathbf{j}$ instead of $\mathbf{j}$ in (41), then it's better *not* to gauge [80]. ♢

This is not all. If we refrain to eliminate $\mathbf{h}$ in the reduction from (39) to (41), but still set $\mathbf{b} = \mathbf{R}\mathbf{a}$, we get an intermediate two-equation system,

$$\begin{pmatrix} -\boldsymbol{\mu} & \mathbf{R} \\ \mathbf{R}^t & 0 \end{pmatrix} \begin{pmatrix} \mathbf{h} \\ \mathbf{a} \end{pmatrix} = \begin{pmatrix} 0 \\ \mathbf{j} \end{pmatrix}, \tag{42}$$

often called a *mixed* algebraic system [3]. (Again, little interest if $\boldsymbol{\mu}$ is full, i.e., unless $\boldsymbol{\nu}$ was diagonal from the outset.) The same manipulation in the other direction (eliminating $\mathbf{h}$ by $\mathbf{h} = \mathbf{h}^\mathbf{j} + \mathbf{D}^t\boldsymbol{\varphi}$, but keeping $\mathbf{b}$) gives

$$\begin{pmatrix} -\boldsymbol{\nu} & \mathbf{D}^t \\ \mathbf{D} & 0 \end{pmatrix} \begin{pmatrix} \mathbf{b} \\ \boldsymbol{\varphi} \end{pmatrix} = \begin{pmatrix} -\mathbf{h}^\mathbf{j} \\ 0 \end{pmatrix}. \tag{43}$$

[41] Alternatively (and this is how non-homogeneous boundary conditions can be handled), one may work with enlarged incidence matrices $\mathbf{R}$ and $\mathbf{D}$ and enlarged DoF arrays, taking all cells into account, then assign boundary values to passive cells, and keep only active DoFs on the left-hand side.

[42] There are such arrays, owing to $\mathbf{G}^t\mathbf{j} = 0$, because $\ker(\mathbf{G}^t) = \operatorname{cod}(\mathbf{R}^t)$, by transposition of $\operatorname{cod}(\mathbf{G}) = \ker(\mathbf{R})$, in the simple situation we consider. Finding one is an easy task, which does not require solving a linear system. Also by transposition of $\operatorname{cod}(\mathbf{R}) = \ker(\mathbf{D})$, one has $\ker(\mathbf{R}^t) = \operatorname{cod}(\mathbf{D}^t)$, and hence $\mathbf{R}^t(\mathbf{h} - \mathbf{h}^\mathbf{j}) = 0$ implies $\mathbf{h} = \mathbf{h}^\mathbf{j} + \mathbf{D}^t\boldsymbol{\varphi}$.

[43] It stems from $\ker(\mathbf{D}^t) = 0$. Indeed, $\mathbf{D}^t\boldsymbol{\psi} = 0$ means that $\Sigma_v \mathbf{D}^f_v \boldsymbol{\psi}_v = 0$ for all primal facets f. For some facets (those in Σ^h), there is but *one* volume v such that $\mathbf{D}^f_v \neq 0$, which forces $\boldsymbol{\psi}_v = 0$ for this v. Remove all such volumes v, and repeat the reasoning and the process, thus spreading the value 0 to all $\boldsymbol{\psi}_v$s.

We are not yet through. There is an interesting variation on (43), known as the mixed-hybrid approach. It's a kind of "maximal domain decomposition", in the sense that all volumes are made independent by "doubling" the degrees of freedom of $\mathbf{b}$ and $\mathbf{h}$ (two distinct values on sides of each facet not in Σ^h). Let's redefine the enlarged arrays and matrices accordingly, and call them $\overline{\mathbf{b}}, \overline{\mathbf{h}}, \overline{\boldsymbol{\nu}}, \overline{\mathbf{D}}, \overline{\mathbf{R}}$. Constraints on $\overline{\mathbf{b}}$ (equality of up- and downstream fluxes) can be expressed as $\mathbf{N}\overline{\mathbf{b}} = 0$, where $\mathbf{N}$ has very simple structure (one 1×2 block, with entries 1 and -1, for each facet). Now, introduce an array $\mathbb{\lambda}$ of facet-based Lagrange multipliers, and add $(\mathbb{\lambda}, \mathbf{N}\overline{\mathbf{b}})$ to the underlying Lagrangian of (43). This gives a new discrete formulation (still equivalent to (39), if one derives $\mathbf{b}$ and $\mathbf{h}$ from $\overline{\mathbf{b}}$ and $\overline{\mathbf{h}}$ the obvious way):

$$\begin{pmatrix} -\overline{\boldsymbol{\nu}} & \overline{\mathbf{D}}^t & \mathbf{N}^t \\ \overline{\mathbf{D}} & 0 & 0 \\ \mathbf{N} & 0 & 0 \end{pmatrix} \begin{pmatrix} \overline{\mathbf{b}} \\ \boldsymbol{\varphi} \\ \mathbb{\lambda} \end{pmatrix} = \begin{pmatrix} -\overline{\mathbf{h}}^{\mathrm{j}} \\ 0 \\ 0 \end{pmatrix}.$$

Remark that the enlarged $\overline{\boldsymbol{\nu}}$ is block-diagonal (as well as its inverse $\overline{\boldsymbol{\mu}}$), hence easy elimination of $\overline{\mathbf{b}}$. What then remains is a symmetric system in $\boldsymbol{\varphi}$ and $\boldsymbol{\lambda}$:

$$\begin{pmatrix} \overline{\mathbf{D}}\overline{\boldsymbol{\mu}}\overline{\mathbf{D}}^t & \overline{\mathbf{D}}\overline{\boldsymbol{\mu}}\mathbf{N}^t \\ \mathbf{N}\overline{\boldsymbol{\mu}}\overline{\mathbf{D}}^t & \mathbf{N}\overline{\boldsymbol{\mu}}\mathbf{N}^t \end{pmatrix} \begin{pmatrix} \boldsymbol{\varphi} \\ \boldsymbol{\lambda} \end{pmatrix} = - \begin{pmatrix} \overline{\mathbf{D}}\overline{\boldsymbol{\mu}}\overline{\mathbf{h}}^{\mathrm{j}} \\ \mathbf{N}\overline{\boldsymbol{\mu}}\overline{\mathbf{h}}^{\mathrm{j}} \end{pmatrix}.$$

The point of this manipulation is that $\overline{\mathbf{D}}\overline{\boldsymbol{\mu}}\overline{\mathbf{D}}^t$ is *diagonal*, equal to $\mathbf{K}$, say. So we may again eliminate $\boldsymbol{\varphi}$, which leads to a system in terms of only $\boldsymbol{\lambda}$:

$$\mathbf{N}[\overline{\boldsymbol{\mu}} - \overline{\boldsymbol{\mu}}\overline{\mathbf{D}}^t\mathbf{K}^{-1}\overline{\mathbf{D}}\overline{\boldsymbol{\mu}}]\mathbf{N}^t\boldsymbol{\lambda} = \mathbf{N}[\overline{\boldsymbol{\mu}}\overline{\mathbf{D}}^t\mathbf{K}^{-1}\overline{\mathbf{D}}\overline{\boldsymbol{\mu}} - \overline{\boldsymbol{\mu}}]\overline{\mathbf{h}}^{\mathrm{j}}. \tag{44}$$

Contrived as it may look, (44) is a quite manageable system, with a sparse symmetric matrix. (The bracketed term on the left is block-diagonal, like $\overline{\boldsymbol{\mu}}$.)

Remark. In $(\mathbb{\lambda}, \mathbf{N}\overline{\mathbf{b}})$, each $\boldsymbol{\lambda}_f$ multiplies a term $(\mathbf{N}\overline{\mathbf{b}})_f$ which is akin to a magnetic charge. Hence the $\boldsymbol{\lambda}_f$s should be interpreted as facet-DoFs of a magnetic potential, which assumes the values necessary to reestablish the equality between fluxes that has been provisionally abandoned when passing from $\mathbf{b}$ to the enlarged (double size) flux vector $\overline{\mathbf{b}}$. $\diamondsuit$

There is a dual mixed-hybrid approach, starting from (42), where *dual* volumes are made independent, hence (in the case of a simplicial primal mesh) three DoF's per facet, for both $\mathbf{b}$ and $\mathbf{h}$, and two Lagrange multipliers to enforce their equality. This leads to a system similar to (44)—but with twice as many unknowns, which doesn't make it attractive.

Systems (40), (41), (42), (43) and (44) all give the same solution pair $\{\mathbf{b}, \mathbf{h}\}$. Which one effectively to solve, therefore, is uniquely a matter of algorithmics, in which size, sparsity, and effective conditioning should be considered. The serious contenders are the one-matrix semi-definite systems, i.e., (40), (41), and (44). An enumeration of the number of off-diagonal terms (which is a fair figure of merit when using conjugate gradient methods on such matrices), shows that (44) rates better than (41), as a rule. The block-centered scheme (40) outperforms both (41) and (44), but is not available[44] with the Galerkin hodge. Hence the enduring interest [24, 56, 71, 47] for the "mixed-hybrid" method (44).

Each of the above schemes could be presented as the independent discretization of a specific mixed or mixed-hybrid variational formulation, and the literature is replete with sophisticated analyses of this kind. Let's reemphasize that all these schemes are *algebraically* equivalent, as regards $\mathbf{b}$ and $\mathbf{h}$. Therefore, an error analysis of one of them applies to all: For instance, if $\boldsymbol{\nu}$ is the Galerkin hodge, the standard variational convergence proof for (41), or if $\boldsymbol{\mu}$ is the diagonal hodge of (34), the error analysis we shall perform next Section, on the symmetrical system (39).

[44] unless one messes up with the computation of the terms of the mass-matrix, by using ad-hoc approximate integration formulas. This is precisely one of the devices used in mass-lumping.

3.7 Playing with the kit: Miscellanies

The advantage of working at the discrete level from the outset is confirmed by most examples one may tackle. For instance, the discrete version of the eddy-current problem (29) is, without much ado, found to be

$$i\omega\boldsymbol{\sigma}\mathbf{E} + \mathbf{R}^t\boldsymbol{\nu}\mathbf{R}\,\mathbf{E} = -i\omega\mathbf{J}^s. \tag{45}$$

As a rule, σ vanishes outside of a closed region $C = D - \Delta$ of the domain, C for "conductor". (Assume, then, that A, which is $\mathrm{supp}(\mathbf{J}^s)$, is contained in Δ.) The system matrix then has a non-trivial null space, $\ker(\boldsymbol{\sigma}) \cap \ker(\mathbf{R})$, and uniqueness of $\mathbf{E}$ is lost. It can be restored by enforcing the constraint $\mathbf{G}^t\boldsymbol{\epsilon}_\Delta\mathbf{E} = 0$, where $\boldsymbol{\epsilon}_\Delta$ is derived from $\boldsymbol{\epsilon}$ by setting to zero all rows and columns which correspond to edges borne by C. Physically, this amounts to assume a zero electric charge density outside the conductive region $C = \mathrm{supp}(\sigma)$. (Beware, the electric field obtained this way can be seriously wrong about A, where this assumption is not warranted, in general. However, the electric field on C is correct.) Mathematically, the effect is to limit the span of the unknown $\mathbf{E}$ to a subspace over which $i\omega\boldsymbol{\sigma} + \mathbf{R}^t\boldsymbol{\nu}\mathbf{R}$ is regular.

In some applications, however, the conductivity is nonzero in all D, but may assume values of highly different magnitudes, and the above matrix, though regular, is ill-conditioned. One then will find in the kit the right tools to "regularize" such a "stiff" problem. See [25] for an example of the procedure, some aspects of which are studied in detail in [16]. Briefly, it consists in adding to the left-hand side of (45) a term, function of $\mathbf{E}$, that vanishes when $\mathbf{E}$ is one of the solutions of (45), which supplements the $\mathbf{R}^t\boldsymbol{\nu}\mathbf{R}$ matrix by, so to speak, what it takes to make it regular (and hence, to make the whole system matrix well conditioned, however small σ can be at places). The modified system is

$$i\omega\boldsymbol{\sigma}\mathbf{E} + \mathbf{R}^t\boldsymbol{\nu}\mathbf{R}\,\mathbf{E} + \boldsymbol{\sigma}\mathbf{G}\boldsymbol{\delta}\mathbf{G}^t\boldsymbol{\sigma}\mathbf{E} = -i\omega\mathbf{J}^s, \tag{46}$$

where $\boldsymbol{\delta}$ is a Hodge-like matrix, node based, diagonal, whose entries are $\boldsymbol{\delta}^{nn} = \int_{\tilde{n}} 1/\mu\sigma^2$. A rationale for this can be found in [16]: In a nutshell, the idea is to "load the null space" of $\mathbf{R}^t\boldsymbol{\nu}\mathbf{R}$, and dimensional considerations motivate the above choice of $\boldsymbol{\delta}$. Our sole purpose here is to insist that all this can be done at the discrete level.

Remark. One *might* motivate this procedure by starting from the following equation, here obtained from (46) by simply using the toolkit in the other direction ("discrete" to "continuous"):

$$i\omega\sigma\mathrm{E} + \mathrm{rot}(\nu\,\mathrm{rot}\,\mathrm{E}) - \sigma\,\mathrm{grad}(\frac{1}{\mu\sigma^2}\,\mathrm{div}(\sigma\mathrm{E})) = -i\omega\mathrm{J}^s, \tag{47}$$

but which can be seen as a natural regularization of (29). (We revert to vector proxies here to call attention on the use of a variant of the $-\Delta = \mathrm{rot}\circ\mathrm{rot} - \mathrm{grad}\circ\mathrm{div}$ formula, which is relevant when both μ and σ are uniform in (47).) This is a time-honored idea [63]. Part of its present popularity may stem from its allowing standard discretization via *node-based* vector-valued elements (the discrete form is then of course quite different[45] from (46)), because E in (47) has more a priori regularity than E in (29). Even if one has reasons to prefer using such elements, the advantage is only apparent, because the discrete solution may converge towards something else than the solution of (29) in some cases (e.g., reentrant corners, cf. [27]), where the solution of (45) has *too much* regularity to satisfy (29). This should make one wary of this approach. $\Diamond$

Many consider the nullspace of $\mathbf{R}^t\boldsymbol{\nu}\mathbf{R}$ as a matter of concern, too, as regards the eigenmode problem,

$$\mathbf{R}^t\boldsymbol{\nu}\mathbf{R}\,\mathbf{E} = \omega^2\boldsymbol{\epsilon}\,\mathbf{E}, \tag{48}$$

[45] When σ and ν are the Galerkin hodges, (46) corresponds to the edge-element discretization of (47).

because $\omega = 0$ is an eigenvalue of multiplicity N (the number of active nodes). Whether the concern is justified is debatable, but again, there are fixing tools in the kit. First, regularization, as above:

$$[\mathbf{R}^t\boldsymbol{\nu}\mathbf{R} + \boldsymbol{\epsilon}\,\mathbf{G}\boldsymbol{\delta}\mathbf{G}^t\boldsymbol{\epsilon}]\mathbf{E} = \omega^2\boldsymbol{\epsilon}\,\mathbf{E}, \tag{49}$$

with $\delta^{nn} = \int_{\tilde{n}} 1/\mu\epsilon^2$ this time. Zero is not an eigenvalue any longer, but new eigenmodes appear, those of $\boldsymbol{\epsilon}\,\mathbf{G}\boldsymbol{\delta}\mathbf{G}^t\boldsymbol{\epsilon}\;\mathbf{E} = \omega^2\boldsymbol{\epsilon}\,\mathbf{E}$ under the restriction $\mathbf{E} = \mathbf{G}\boldsymbol{\psi}$. As remarked in [108], we have here (again, assuming uniform coefficients) a phenomenon of "spectral complementarity" between the operators rot $\circ$ rot and $-$ grad $\circ$ div. The new modes, or "ghost modes" [105], have to be sifted out, which is in principle easy[46] (evaluate the norm $|\mathbf{G}^t\boldsymbol{\epsilon}\,\mathbf{E}|_\delta$), or "swept to the right" by inserting an appropriate scalar factor in front of the regularizing term. Second solution [100]: Restrict the search of $\mathbf{E}$ to a complement of $\ker(\mathbf{R}^t\boldsymbol{\nu}\mathbf{R})$, which one can do by so-called "tree-cotree" techniques [1, 73]. This verges on the issue of *discrete Helmholtz decompositions,* another important tool in the kit, which cannot be given adequate treatment here (see [79]).

[46] These ghost modes are *not* the (in)famous "spurious modes" which were such a nuisance before the advent of edge elements [11]. Spurious modes occur when one solves the eigenmode problem $\mathrm{rot}(\nu\,\mathrm{rot}\,\mathrm{E}) = \omega^2\epsilon\mathrm{E}$ by using *nodal vectorial* elements. Then (barring exceptional boundary conditions) the rot(ν rot) matrix is regular (because the approximation space does not contain gradients, contrary to what happens with edge elements), but also—and for the same reason, as explained in [12]—poorly conditioned, which is the root of the evil. It would be useful *not* to take "ghost modes" and "spurious modes" as synonyms, in order to avoid confusion on this tricky point.